Check for updates

Received: 3 August 2023 | Revised: 27 December 2023 | Accepted: 20 February 2024

DOI: 10.1111/apha.14124

ACTA PHYSIOLOGICA

RESEARCH PAPER

Impairment of the adrenergic reserve associated with exercise intolerance in a murine model of heart failure with preserved ejection fraction

Lukas Semmler[1,2] | **Tobias Jeising**[1,2] | **Judith Huettemeister**[1,2] | **Marc Bathe-Peters**[3,4] | **Konstantina Georgoula**[3] | **Rashin Roshanbin**[1] | **Paulina Sander**[1,2] | **Shu Fu**[1,2] | **David Bode**[1,2] | **Felix Hohendanner**[1,2] | **Burkert Pieske**[5] | **Paolo Annibale**[3,4] | **Gabriele G. Schiattarella**[1,2,6] | **Christian U. Oeing**[1,2] | **Frank R. Heinzel**[1,2,7]

[1]Department of Internal Medicine and Cardiology, German Heart Center Charité (DHZC) – Campus Virchow-Klinikum, Berlin, Germany

[2]German Center for Cardiovascular Research (DZHK), Partner Site Berlin, Berlin, Germany

[3]Receptor Signalling Group, Max Delbrück Center for Molecular Medicine in the Helmholtz Association (MDC), Berlin, Germany

[4]School of Physics and Astronomy, University of St Andrews, St Andrews, UK

[5]Division of Cardiology, Department of Internal Medicine, University Medicine Rostock, Rostock, Germany

[6]Translational Approaches in Heart Failure and Cardiometabolic Disease, Max Delbrück Center for Molecular Medicine in the Helmholtz Association (MDC), Berlin, Germany

[7]2. Medizinische Klinik – Kardiologie, Angiologie, Intensivmedizin, Städtisches Klinikum Dresden, Dresden, Germany

Correspondence
Frank R. Heinzel, Department of Internal Medicine and Cardiology, German Heart Center Charité (DHZC) – Campus Virchow-Klinikum, Berlin 13353, Germany.
Email: frank.heinzel@klinikum-dresden.de

Funding information
Deutsche Forschungsgemeinschaft, Grant/Award Number: SFB1470; Deutsches Zentrum für Herz-Kreislaufforschung

Abstract

Aim: Exercise intolerance is the central symptom in patients with heart failure with preserved ejection fraction. In the present study, we investigated the adrenergic reserve both in vivo and in cardiomyocytes of a murine cardiometabolic HFpEF model.

Methods: 12-week-old male C57BL/6J mice were fed regular chow (control) or a high-fat diet and L-NAME (HFpEF) for 15 weeks. At 27 weeks, we performed (stress) echocardiography and exercise testing and measured the adrenergic reserve and its modulation by nitric oxide and reactive oxygen species in left ventricular cardiomyocytes.

Results: HFpEF mice (preserved left ventricular ejection fraction, increased E/e′, pulmonary congestion [wet lung weight/TL]) exhibited reduced exercise capacity and a reduction of stroke volume and cardiac output with adrenergic stress. In ventricular cardiomyocytes isolated from HFpEF mice, sarcomere shortening had a higher amplitude and faster relaxation compared to control animals. Increased shortening was caused by a shift of myofilament calcium sensitivity.

Christian U. Oeing and Frank R. Heinzel have contributed equally to the manuscript.

This is an open access article under the terms of the Creative Commons Attribution-NonCommercial-NoDerivs License, which permits use and distribution in any medium, provided the original work is properly cited, the use is non-commercial and no modifications or adaptations are made.
© 2024 The Authors. *Acta Physiologica* published by John Wiley & Sons Ltd on behalf of Scandinavian Physiological Society.

With addition of isoproterenol, there were no differences in sarcomere function between HFpEF and control mice. This resulted in a reduced inotropic and lusitropic reserve in HFpEF cardiomyocytes. Preincubation with inhibitors of nitric oxide synthases or glutathione partially restored the adrenergic reserve in cardiomyocytes in HFpEF.

Conclusion: In this murine HFpEF model, the cardiac output reserve on adrenergic stimulation is impaired. In ventricular cardiomyocytes, we found a congruent loss of the adrenergic inotropic and lusitropic reserve. This was caused by increased contractility and faster relaxation at rest, partially mediated by nitro-oxidative signaling.

KEYWORDS

adrenergic signaling, cardiac output reserve, exercise intolerance, heart failure with preserved ejection fraction, nitro-oxidative signaling

1 | INTRODUCTION

Exercise intolerance in patients with heart failure with preserved ejection fraction (HFpEF) severely limits quality of life, independently predicts mortality, and remains extremely difficult to treat.[1] Reduced peripheral oxygen extraction and a reduction of cardiac output during exercise have been observed in patients with HFpEF.[2] Both chronotropic incompetence and a reduction of the indexed stroke volume during exercise predicted exercise intolerance in patients with HFpEF in a recent meta-analysis.[2] While sinoatrial node dysfunction has recently been discovered as one underlying pathology causing chronotropic incompetence,[3] the mechanisms underlying the loss of stroke volume during exercise in HFpEF patients are insufficiently understood. In patients with Heart Failure with Reduced Ejection Fraction (HFrEF), deficits of the adrenergic signaling pathway contribute to the loss of adrenergic reserve in cardiomyocytes and hence the loss of cardiac output reserve.[4] However, little is known about this signaling pathway and its influence on exercise intolerance in HFpEF.

It has recently been shown that Nitric oxide (NO) is a modulator of the adrenergic response in cardiomyocytes.[5,6] NO exerts its regulatory function via two mechanisms: (1) activation of the soluble guanylyl cyclase (sGC), subsequent synthesis of cyclic guanosine monophosphate (cGMP), activation of the cGMP-dependent protein kinase (PKG) and phosphorylation of substrates and (2) direct S-nitrosylation of cysteine residues and hence post-translational regulation of protein activity. S-nitrosylation of phospholamban, ryanodine receptor, and cardiac troponin C induced by adrenergic stimulation acts in concert with phosphorylation and is required to recruit the maximal adrenergic reserve.[5,6] Interestingly, two independent research groups found evidence of dysregulation of NO signaling and especially S-nitrosylation in HFpEF.[7,8] However, the impact on cellular contractility, calcium handling and the adrenergic reserve in HFpEF has not yet been investigated. This modulation complements the long-established β1 (β1-AR) and β2 adrenergic receptor-mediated modulation of inotropic and lusitropic responses.

We therefore hypothesize that a deficit of the adrenergic reserve in cardiomyocytes contributes to the loss of cardiac output reserve and hence exercise intolerance in HFpEF. We systematically investigated the organ and cardiomyocyte reaction to adrenergic stimuli in a murine model of HFpEF. Given its representation of typical HFpEF clinical features and its widespread use in HFpEF research, we selected a murine model feeding a high-fat diet combined with Nω-Nitro-L-arginine (L-NAME) in drinking water. Considering the role of NO in cardiac excitation-contraction coupling[5] and recent discoveries about its dysregulation in HFpEF,[7,8] we further studied the molecular effects of NO on the adrenergic reserve in HFpEF.

2 | RESULTS

2.1 | In vivo cardiac dysfunction with isoproterenol stress

After 15 weeks of L-NAME and HFD (Figure 1A), mice exhibited an HFpEF phenotype evident as (1) concentric hypertrophy with preserved left ventricular (LV) ejection fraction (Figure 1B–E, Supporting Information Table S1), (2) impaired diastolic function (Figure 1F,G) and (3) lung edema as a sign of pulmonary congestion (Figure 1H).

17481716, 0, Downloaded from https://onlinelibrary.wiley.com/doi/10.1111/apha.14124 by University Of St Andrews University, Wiley Online Library on [04/03/2024]. See the Terms and Conditions (https://onlinelibrary.wiley.com/terms-and-conditions) on Wiley Online Library for rules of use; OA articles are governed by the applicable Creative Commons License

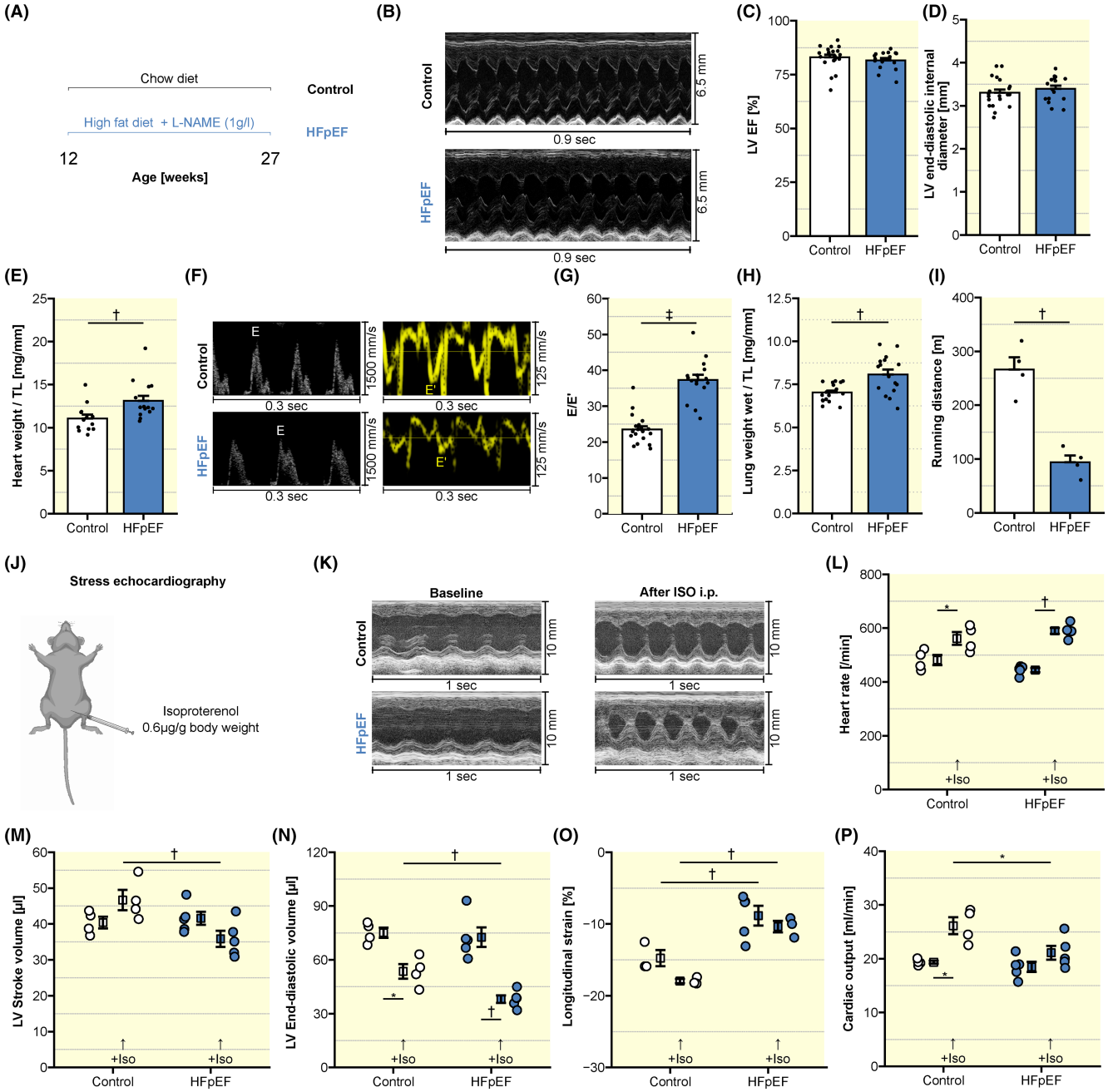

FIGURE 1 HFpEF mice show dysfunction on Iso stress echocardiography. (A) Experimental design. 12 weeks old, male C57BL6/J mice were fed regular chow diet and standard water or high-fat diet and 1 g/L L-NAME via the drinking water for 15 weeks. All further experiments were conducted after 15 weeks. (B) Representative left ventricular M-mode echocardiography image from the short parasternal axis view. (C) Left ventricular ejection fraction calculated from M-mode images. (D) Left ventricular end-diastolic internal diameter from M-mode images. (E) Heart weight divided by tibial length. (F) Representative images of pulse-wave Doppler images of the mitral valve flow (left) and tissue Doppler imaging of the mitral valve annulus (right). (G) Ratio of mitral valve E and E′ wave. (H) Ratio of the wet lung weight and tibial length. (I) Maximum running distance on a treadmill exercise-exhaustion test. (J) Iso stress echocardiography protocol. For details, see Methods. (K) Representative left ventricular M-mode echocardiographic image from the long parasternal axis view at rest and after Iso injection. (L) Heart rate before and after administration of Iso. (M) Stroke volume before and after administration of isoproterenol. (N) End-diastolic volume before and after administration of Iso. (O) Longitudinal strain before and after administration of Iso. (P) Cardiac output before and after administration of Iso. Unpaired Student's *t*-test (C–E, G–I). Mixed effect model for repeated measure data followed by Sidak-controlled post-hoc testing (I–P). Data are expressed as mean ± SEM. $^{*}p < 0.05$, $^{\dagger}p < 0.01$, and $^{\ddagger}p < 0.001$.

17481716, 0, Downloaded from https://onlinelibrary.wiley.com/doi/10.1111/apha.14124 by University Of St Andrews University, Wiley Online Library on [04/03/2024]. See the Terms and Conditions (https://onlinelibrary.wiley.com/terms-and-conditions) on Wiley Online Library for rules of use; OA articles are governed by the applicable Creative Commons License

Importantly, maximum running distance was drastically impaired (Figure 1I).

On stress echocardiography, HFpEF and control mice exhibited comparable increases in heart rate with isoproterenol (Iso) (Figure 1J–L). While stroke volumes were similar at rest, the increase of stroke volume with Iso was lost in HFpEF and mice had drastically lower stroke volumes compared to control animals (Figure 1M). This was caused by a reduction of end-diastolic volume during adrenergic stress in HFpEF compared with control (Figure 1N). Interestingly, both end-systolic volumes and ejection fraction changed similarly between groups besides severe impairments of the longitudinal strain (Figure 1O, Supporting Information Figure S1A,B). Subsequently, the increase of cardiac output with adrenergic stimuli observed in control mice was lost in HFpEF mice (Figure 1P).

2.2 | Impaired sarcomeric adrenergic reserve

We next assessed whether the loss of adrenergic reserve in HFpEF mice in vivo could be related to changes in sarcomere shortening in adult, ventricular cardiomyocytes (AVCMs). HFpEF cardiomyocytes were hypercontractile at baseline evident as an increased amplitude of sarcomere shortening and a faster relaxation (Figure 2A–D). To ensure these findings are not specific to the two-hit mouse model, we further confirmed these in obese Zucker fatty and spontaneously hypertensive (ZSF1) rats, a well-established rat model of cardiometabolic HFpEF. There, we found faster relaxation but did not see a significant increase in sarcomere shortening amplitude (Supporting Information Figure S2). After the addition of Iso, amplitude and kinetics reached similar maximal levels in both groups (Figure 2B,D). Accordingly, the lusitropic reserve was reduced in HFpEF, there was less acceleration of the contraction and we saw a tendency towards a reduction in inotropic reserve in HFpEF (Figure 2C,E,G). Diastolic sarcomere length at rest and after Iso was not changed (Figure 2H). Intriguingly, the degree of diastolic dysfunction (E/e′) on echocardiography correlated inversely with the duration of sarcomere relaxation (Figure 2I).

2.3 | Faster calcium reuptake and increased myofilament sensitivity

To better understand the changes of sarcomere shortening in AVCMs we studied cellular calcium handling. Calcium transient amplitude at baseline was not altered but the amplitude after the addition of Iso was reduced in HFpEF (Figure 3A,B). Accordingly, the increase of the calcium transient amplitude with Iso was reduced in AVCMs isolated from HFpEF mice (Figure 3C). Calcium transient decay was accelerated in HFpEF at rest and after the addition of Iso, both groups reached comparable kinetics of calcium reuptake (Figure 3D). Again, lusitropic reserve was significantly reduced in HFpEF (Figure 3E). There was a fine correlation between calcium reuptake and sarcomere shortening on a single cardiomyocyte base, which supports the role of accelerated calcium reuptake in mediating faster sarcomere relaxation (Figure 3F). In the presence of unaltered calcium amplitude, changes in calcium sensitivity could account for the increased sarcomere shortening amplitude in HFpEF. We calculated the first derivative of sarcomere shortening over calcium reuptake at 50% sarcomere relaxation, a well-established parameter of calcium sensitivity.[9] Indeed, this parameter was increased in HFpEF AVCMs (Figure 3G,H). In combination with unaltered diastolic calcium levels (Figure 3I), this indicates a higher calcium sensitivity explaining the increased sarcomere shortening amplitude.

We further investigated calcium handling in the sarcoplasmic reticulum compartment as previously described (Figure 3J).[10] We did not find differences in the sarcoplasmic reticulum calcium load, measured as the amplitude of the calcium transient caused by rapid perfusion with caffeine (Figure 3K). However, the decay constant of the caffeine-induced transient was drastically increased in HFpEF AVCMs (Figure 3L). This indicates a reduced activity of the sodium–calcium exchanger (NCX) in forward mode Although the overall proportion of cells with spontaneous calcium release events (CaREv, waves, and sparks) was unaltered, the frequency of waves in cells with CaREv was significantly increased in HFpEF in comparison to control (Figure 3M,N).

2.4 | β-adrenergic signaling pathway

In order to explain the reduced calcium transient amplitude after isoproterenol stimulation in HFpEF AVMCs we investigated the membrane expression of the most abundant adrenoreceptor, namely the β1-AR. Using fluorescence correlation spectroscopy of a fluorescent β1-AR agonist, we did not find a difference in the density of β1-AR on the outer membrane of AVMC (Figure 4A,B).

To investigate the molecular mechanisms of the accelerated calcium reuptake in HFpEF cardiomyocytes, we investigated the expression and phosphorylation of the main proteins involved. We did not see a change in SERCA2 expression but a trend toward increased phospholamban

17481716, 0, Downloaded from https://onlinelibrary.wiley.com/doi/10.1111/apha.14124 by University Of St Andrews University, Wiley Online Library on [04/03/2024]. See the Terms and Conditions (https://onlinelibrary.wiley.com/terms-and-conditions) on Wiley Online Library for rules of use; OA articles are governed by the applicable Creative Commons License

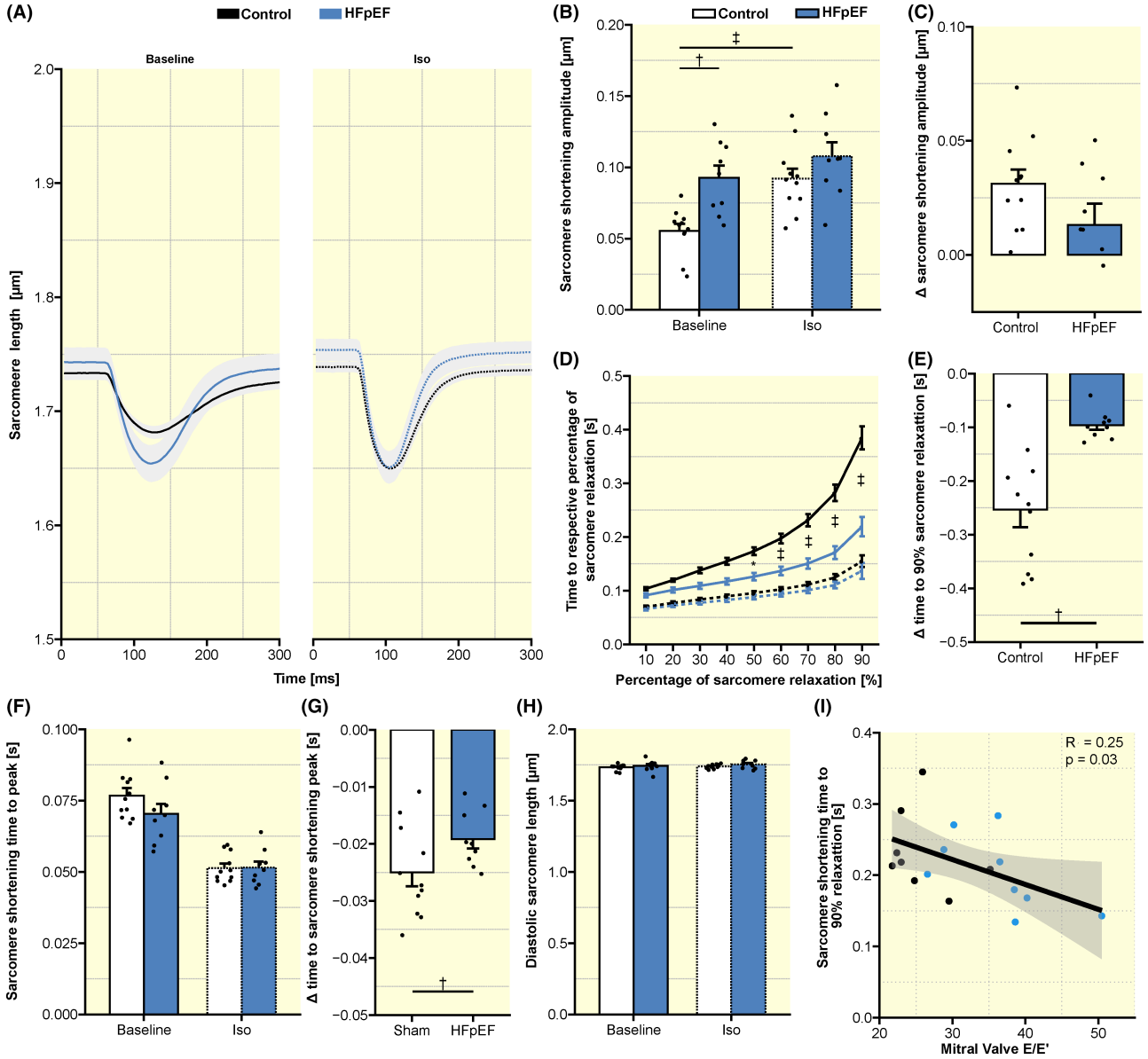

FIGURE 2 Sarcomere shortening adrenergic reserve is impaired in HFpEF cardiomyocytes. (A) Averaged sarcomere shortening trace before and after the administration of Iso. (B) Sarcomere shortening amplitude. (C) Change of sarcomere shortening amplitude after the administration of Iso. (D) Sarcomere relaxation times before and after the administration of Iso. (E) Change the time to 90% relaxation of the sarcomere shortening trace after the administration of Iso. (F) Time to peak of the sarcomere shortening trace. (G) Change of the time to peak of the sarcomere shortening trace after the administration of Iso. (H) Diastolic sarcomere length before and after Iso. (I) Sarcmere shortening in atrial myocytes as a function of E/E'. Data are expressed as mean ± SEM. All statistics were performed per animal, dots represent animal means Unpaired Student's *t*-test (C, E, G). Mixed effect model for repeated measure data followed by Sidak-controlled post-hoc testing (B, D, F, H). $^{*}p<0.05$, $^{\dagger}p<0.01$, and $^{\ddagger}p<0.001$.

expression in HFpEF ($p=0.054$, Supporting Information Figure S3A–C). Additionally, the amount of phospholamban phosphorylated on Ser16 was increased in HFpEF (Supporting Information Figure S3D). Looking at proteins known to regulate the myofilament sensitivity, we did not see a change of total myosin-binding protein C 3 nor the amount that was phosphorylated on Ser282 (Supporting Information Figure S3E–G). The total amount of troponin I was reduced in HFpEF, but the amount of troponin I phosphorylated on Ser23 and Ser24 was unaltered (Supporting Information Figure S3H,I).

2.5 | Altered nitro-oxidative balance in cardiomyocytes

As stated above, NO is an important regulator of sarcomere shortening and calcium handling in AVCMs and

17481716, 0, Downloaded from https://onlinelibrary.wiley.com/doi/10.1111/apha.14124 by University Of St Andrews University, Wiley Online Library on [04/03/2024]. See the Terms and Conditions (https://onlinelibrary.wiley.com/terms-and-conditions) on Wiley Online Library for rules of use; OA articles are governed by the applicable Creative Commons License

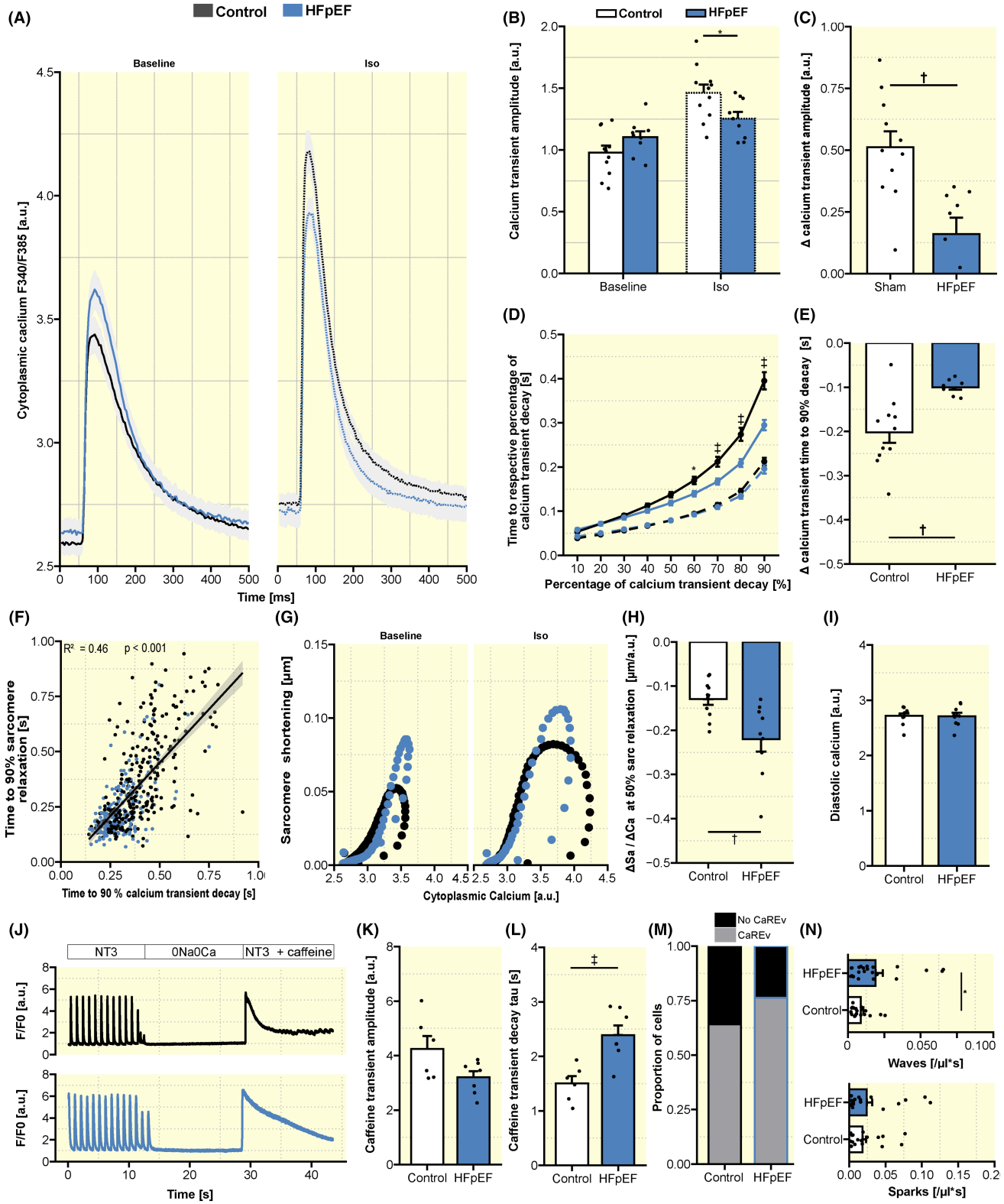

FIGURE 3 Impaired calcium handling and altered myofilament sensitivity underly the deficit of AVCMs contractility. (A) Averaged calcium transient before and after the administration of Iso. (B) Calcium transient amplitude. (C) Change of calcium transient amplitude after the administration of Iso. (D) Calcium transient decay times. (E) Change of the time to 90% decay of the calcium transient after the administration of Iso. (F) Linear regression of the sarcomere shortening trace time to 90% relaxation and calcium transient time to 90% decay. (G) Hysteresis loops before and after the administration of Iso. Data are expressed as mean ± SEM. All statistics (except F, M, N) were performed per animal, dots represent animal means unpaired Student's *t*-test (C, E, H, I, K, L). Chi-squared test (M). Wilcoxon signed-rank test (N). Mixed effect model for repeated measure data followed by Sidak-controlled post-hoc testing (B, D). $^{*}p<0.05$, $^{\dagger}p<0.01$, and $^{\ddagger}p<0.001$.

17481716, 0, Downloaded from https://onlinelibrary.wiley.com/doi/10.1111/apha.14124 by University Of St Andrews University, Wiley Online Library on [04/03/2024]. See the Terms and Conditions (https://onlinelibrary.wiley.com/terms-and-conditions) on Wiley Online Library for rules of use; OA articles are governed by the applicable Creative Commons License

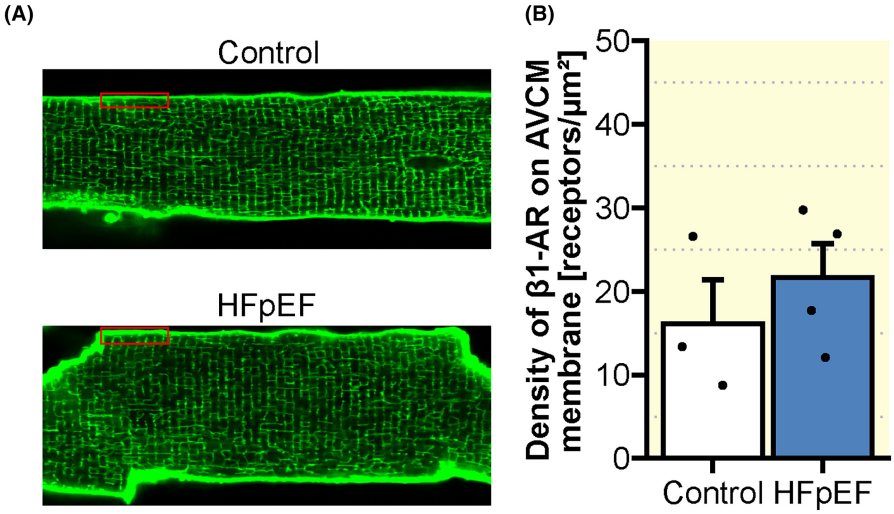

FIGURE 4 Expression of β_1-adrenergic receptors in HFpEF. (A) Representative images of control and HFpEF AVCMs, stained with cell mask green, and the region where the linescans for fluorescence correlation spectroscopy were taken are highlighted in a red box. (B) The number of β_1-adrenergic receptors counted on the outer membrane of AVCM/µm,^{2} based on the extrapolated amplitude G(0) of the autocorrelation function G(tau) of the fluorescence fluctuations at time lag tau = 0 in AVCMs isolated from control (16 cells, 3 mice) and HFpEF (12 cells, 4 mice) mice. All data were analyzed per animal. Data are expressed as mean ± SEM. Unpaired Student's *t*-test (B). $^*p < 0.05$, $^\dagger P < 0.01$, and $^\ddagger p < 0.001$.

was described to be dysregulated in HFpEF. We therefore measured NO release in AVCMs using the highly specific fluorescence probe Cu-FL2 and inhibitors of inducible (iNOS) and neural (nNOS) nitric oxide synthetase.[11] We did not find differences in NO release in non-stimulated AVCMs (Supporting Information Figure S4A). In stimulated cardiomyocytes (5 min 3 Hz), nNOS inhibitor SMTC but neither Iso nor iNOS inhibitor 1400W influenced NO release in AVCM isolated from control (Figure 5A, Supporting Information Figure S4B). In HFpEF AVCMs, Iso increased the NO release and both—SMTC and 1400W—were able to reduce the NO release (Figure 5A, Supporting Information Figure S4B). The cellular effects of NO (activation of sGC vs direct post-translation modification of proteins via formation of S-nitrosothiols) are directly influenced by the oxidative environment.[12] We therefore also investigated reactive oxygen species (ROS) release and found drastically increased ROS release in HFpEF AVCMs (Figure 5B). Elamipretide—a small peptide that targets mitochondrial ROS release—was able to reduce ROS release only in HFpEF AVCMs implying mitochondria as a source of increased ROS release in HFpEF (Figure 5B).

2.6 | Nitro-oxidative signaling influences cardiomyocyte contractility

We next investigated whether the dysregulation of nitro-oxidative balance affects AVCM's sarcomere shortening and calcium handling using SMTC, 1400W, and a cell-permeable analogous to glutathione which was previously used to reduce S-nitrosylation of proteins (Figure 5C).[13] Except for a tendency toward a reduction of sarcomere shortening amplitude with glutathione at baseline in both groups, sarcomere shortening amplitudes remained unaffected (Supporting Information Figure S4C,D). As has been described previously, nNOS inhibition with SMTC reduced the calcium transient amplitude after the addition of Iso in control AVCMs (Figure 5D,E).[6] In AVCM isolated from HFpEF mice, we saw a reduction of the calcium transient amplitude at baseline with SMTC and glutathione which resulted in an increase of the inotropic reserve with glutathione (Figure 5E,F). Additionally, we saw a shortening of the diastolic sarcomere length at baseline with 1400W and SMTC in the HFpEF group (Supporting Information Figure S4E) besides no changes in diastolic calcium (Supporting Information Figure S4F). The changes in sarcomere shortening and calcium handling with the compounds might be explained by a tendency toward a reduction of calcium sensitivity especially with glutathione (Supporting Information Figure S4G).

All three compounds slowed sarcomere relaxation at baseline in both groups but had little effect on relaxation after Iso (Figure 5G). This led to a significant increase of the lusitropic reserve in HFpEF but not control (Figure 5H). We observed a similar pattern for calcium transient relaxation (Supporting Information Figure S4H,I) leading us to conclude that the observed changes in sarcomere kinetics were once again caused by changes in calcium handling.

17481716, 0, Downloaded from https://onlinelibrary.wiley.com/doi/10.1111/apha.14124 by University Of St Andrews University, Wiley Online Library on [04/03/2024]. See the Terms and Conditions (https://onlinelibrary.wiley.com/terms-and-conditions) on Wiley Online Library for rules of use; OA articles are governed by the applicable Creative Commons License

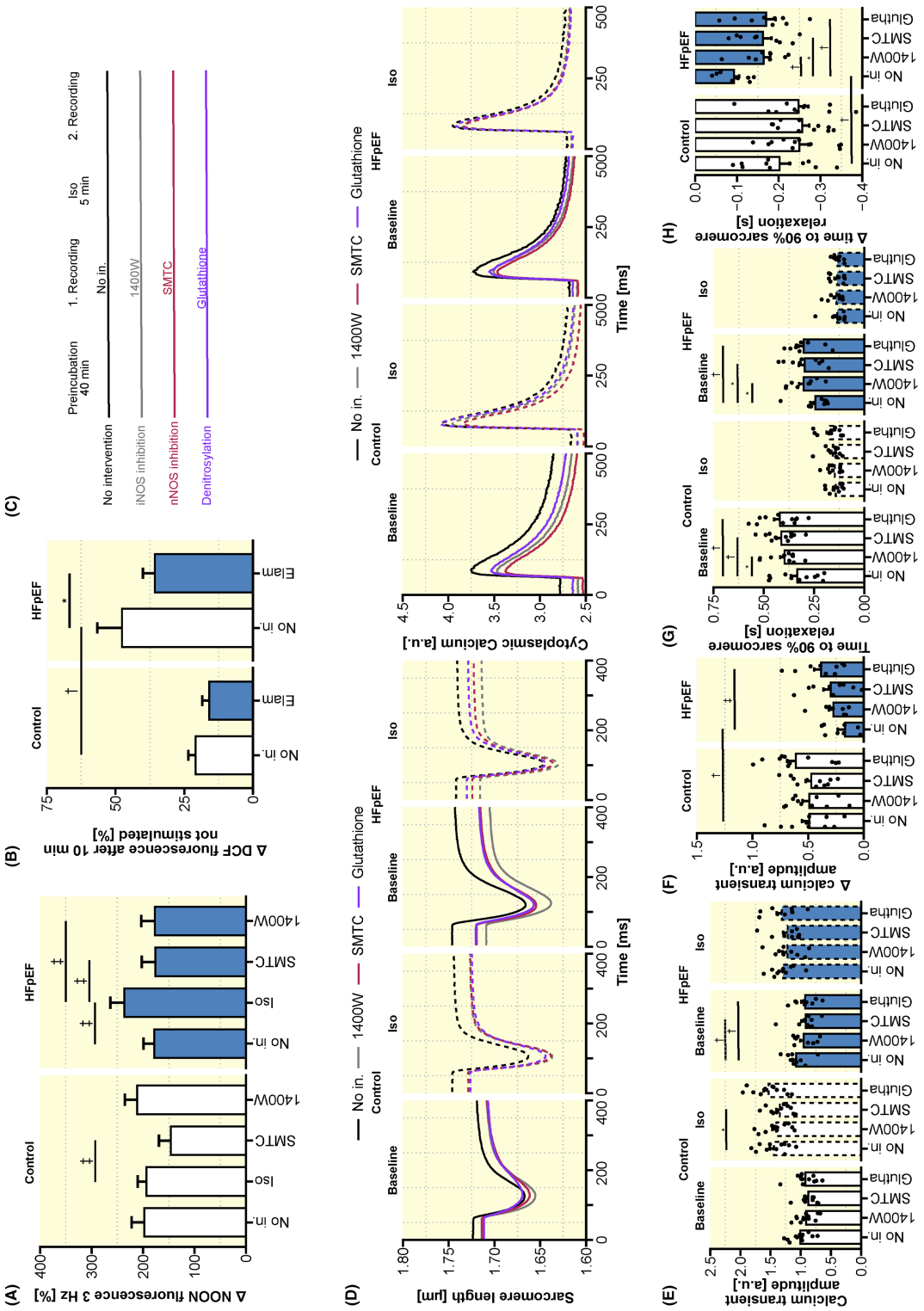

FIGURE 5 Upregulation of nitro-oxidative signaling contributes to impaired cardiomyocyte adrenergic reserve. (A) NO release within 5 min of electrical stimulation at 3 Hz. No in. = no intervention. (B) ROS release in non-stimulated cardiomyocytes over 10 min. (C) Experimental design to investigate the influence of iNOS inhibitor 1400 W, nNOS inhibitor SMTC, and glutathione on AVCM function. (D) Average sarcomere shortening traces and calcium transients in AVCM isolated from control or HFpEF before and after the addition of Iso with or without interventions on the NO/ROS axis. (E) Calcium transient amplitude before and after the addition of Iso with or without interventions of the NO axis. (F) Change of calcium transient amplitude after the addition of Iso with or without interventions of the NO axis. (G) Time to 90% sarcomere relaxation before and after the addition of Iso with or without interventions of the NO axis. (H) Change of the time to 90% sarcomere relaxation after the addition of Iso with or without interventions of the NO axis. Data are expressed as mean ± SEM. For A, B, data were analyzed with means per animal and a mixed effect model for repeated measure data followed by Sidak-controlled post-hoc testing. For E–H, data were analyzed per cell in a mixed model for repeated and clustered data (cells clustered within an animal, for details see Methods) followed by Sidak-controlled post-hoc testing. $^{*}p < 0.05$, $^{\dagger}p < 0.01$, and $^{\ddagger}p < 0.001$.

17481716, 0, Downloaded from https://onlinelibrary.wiley.com/doi/10.1111/apha.14124 by University Of St Andrews University, Wiley Online Library on [04/03/2024]. See the Terms and Conditions (https://onlinelibrary.wiley.com/terms-and-conditions) on Wiley Online Library for rules of use; OA articles are governed by the applicable Creative Commons License

Further supporting a hyperactivation of the nitro-oxidative signaling pathway in HFpEF, the cellular lusitropic response to the NO donor SNAP was reduced in HFpEF AVCMs (Supporting Information Figure S5A–C).

3 | DISCUSSION

Here, we show for the first time a deficit of the adrenergic signaling pathway in vivo and the underlying loss of adrenergic reserve in ventricular cardiomyocytes in a murine model of HFpEF. In contrast to HFrEF, this loss is caused by a hypercontractile state in cardiomyocytes at rest. In addition, we show that the hypercontractile state in cardiomyocytes is partially caused by a shift in the nitro-oxidative balance.

A reduction of cardiac output on exercise is consistently observed in patients with HFpEF and is an important predictor of exercise intolerance and mortality.[2,14–16] However, little is known about the underlying mechanisms. Using stress echocardiography with isoproterenol injection, we assessed the adrenergic axis—a central signaling pathway that increases cardiac output on exercise. In a well-established mouse model of HFpEF with severe exercise intolerance, we found a loss of the cardiac output reserve with adrenergic stimuli. A loss of cardiac output reserve was also seen in patients with HFpEF and has been associated with exercise intolerance in these patients.[2] This strongly suggests that a deficit of the adrenergic axis contributes to the deficits seen in exercise testing. In contrast to previous reports of HFpEF animal models, we did not observe a chronotropic deficit.[3] This might be due to the high dose of isoproterenol that we used to investigate the maximum adrenergic reserve. Instead, loss of cardiac output reserve in HFpEF mice was caused by a reduction of stroke volume with isoproterenol. This was mainly attributable to a loss of end-diastolic volume. Intriguingly, these findings align well with a recent investigation in patients with HFpEF and an ejection fraction above 60%.[17] This specific group of patients was characterized by lower end-diastolic volumes, larger arterial elastance, and a higher end-systolic elastance at rest. On exercise, this group, but not HFpEF patients with an ejection fraction between 50% and 60%, exhibited an inadequate increase of end-diastolic pressure and loss of preload and subsequently stroke volume. Similar changes have already been described in different HFpEF patient cohorts further supporting our findings.[18,19]

In HFrEF, it is well established that the loss of cardiac output with adrenergic stimuli is caused by a deficient adrenergic reserve in cardiomyocytes (as reviewed in Ref. [20]).[4] Here, we show a similar loss of adrenergic reserve in ventricular cardiomyocytes in HFpEF. However, in contrast to HFrEF, the reduced reserve does not result from impairments after adrenergic activation. Instead, we found increased cardiomyocyte contractility, faster relaxation, faster calcium reuptake, and increased calcium myofilament sensitivity at baseline.

Data on cardiomyocyte contractility and calcium handling in HFpEF are not as consistent as in HFrEF. Historically, experiments were first conducted in animal models of left ventricular hypertrophy in response to hypertension without evident diastolic dysfunction. There, a phenotype of largely preserved or even increased cardiomyocyte contractility has been described.[21] Recently, animal models that combine hypertension and metabolic stress have been found to closely resemble the clinical phenotype of HFpEF and their cardiomyocyte function has been investigated (reviewed in Ref. [22]).[7,23] Slowed cardiomyocyte relaxation and delayed calcium reuptake despite equal amplitudes in ZSF1 rats (a model combining genetic risks for obesity and hypertension) has been reported by at least two independent groups.[24,25] Contrary to our study, these experiments were performed using lean ZSF1 rats as controls. These rats are hypertensive and have left ventricular hypertrophy and hypercontractility (increased end-systolic pressure–volume relationship).[23] Cardiomyocytes from animals with left ventricular hypertrophy have been shown to be more contractile (see above). The differences observed in our study may therefore be explained by the different control animals. In Dahl-Salt-sensitive rats (a hypertensive model of HFpEF), Kilfoil et al. reported increased calcium transient amplitudes at baseline but did not report cardiomyocyte contractility.[26] In hypertrophic heart rats (a polygenetic rat model of hypertrophy with diastolic dysfunction in the absence of hypertension), a cardiomyocyte hypercontractile state with accelerated relaxation was observed.[9] In contrast to our results, in that model calcium transient amplitudes were increased and myofilament sensitivity was reduced. In a large animal model of HFpEF combining high-fat diet and aortic banding in Ossabaw swine, the authors also found a hyperdynamic cardiomyocyte phenotype.[27] One study using the same animal model investigated cellular contractility at an early timepoint (after 5 weeks of HFD and L-NAME).[7] At this timepoint, the authors reported partially depressed cardiomyocyte contractility, potentially reflecting a dynamic phenotype during disease progression in which changes in cardiomyocyte contractility dynamically track with the development of the phenotype. Taken together, although less homogenous than in HFrEF, a preserved or even increased basal cardiomyocyte contractility and calcium handling is observed in animal models of HFpEF developing in response to metabolic and hypertensive

17481716, 0, Downloaded from https://onlinelibrary.wiley.com/doi/10.1111/apha.14124 by University Of St Andrews University, Wiley Online Library on [04/03/2024]. See the Terms and Conditions (https://onlinelibrary.wiley.com/terms-and-conditions) on Wiley Online Library for rules of use; OA articles are governed by the applicable Creative Commons License

triggers. Of the very few studies involving human HFpEF tissue, one found an increase in calcium sensitivity similar to our results.[28] To our knowledge, there is no data on the adrenergic reserve in human tissue to date. To further clarify the cardiomyocyte phenotype in HFpEF, more research on human samples will be required.

At first sight, increased cardiomyocyte contractility and faster relaxation seem to oppose the typical presentation of HFpEF patients with increased end-diastolic pressures and exercise intolerance. However, it is well known, that the end-diastolic pressure-volume relationship is influenced by active relaxation and passive properties of the myocardium.[18,29] Both of these properties are closely connected and their individual influence on the end-diastolic volume-pressure relationship is disputed.[18,29] In our mouse model, drastically increased E/e′ in the presence of faster cardiomyocyte relaxation suggests the contribution of passive stiffening (e.g., extracellular fibrosis, intracellular titin modifications). Additional research is required to further define their respective role.

Two independent investigations in HFpEF patients recently found evidence of increased systolic stiffening (measured as the end-systolic pressure–volume relationship) in a subgroup of HFpEF patients characterized by very high ejection fractions (>60% and >65%, respectively).[17,30] Both these studies hypothesized that the increased systolic stiffening is required to maintain sufficient stroke volume besides increased arterial elastance in the HFpEF patients. However, there is a dispute about whether the increased systolic stiffness is caused by active cardiomyocyte contractility or passive tissue properties.[17,30] Although we did not measure arterial elastance, we found unaltered stroke volume, end-diastolic volume, and end-systolic volume in our HFpEF mice besides the presence of hypertension.[7] In analogy to the human findings, it is tempting to hypothesize that the intrinsic cardiomyocyte hypercontractility is a response to increased afterload. However, others have found hypercontractile cardiomyocytes in the absence of increased afterload,[9] indicating hypercontractility may also result from cardiomyocyte remodeling in response to other triggers beyond mechanical load.

In HFrEF, the cardiomyocyte's maximum response to adrenergic stimuli is known to be severely impaired.[4] In contrast, sarcomere shortening amplitudes and kinetics and calcium transient kinetics after the addition of Iso were largely unaffected in this murine HFpEF model. The only deficit we found was a reduced calcium transient amplitude. Very interestingly, Goldhaber et al. found similar results in a rat model of HFpEF.[26] They could further attribute the reduced calcium transient amplitude to a deficit to increase the L-type calcium current with Iso in HFpEF cardiomyocytes. The precise molecular basis of this deficit requires further investigation.

During exercise and at increased heart rates, augmentation of active cardiomyocyte contractility and relaxation is central to maintain low end-diastolic pressures, adequate end-diastolic volumes, and increased cardiac output.[31] Loss of cardiomyocyte inotropic and lusitropic reserve has been demonstrated to underlie the loss of cardiac output reserve in HFrEF.[4] In a recent study of HFpEF patients with an ejection fraction above 60%, an insufficient increase of the end-systolic pressure–volume relationship as well as a loss of recruitable preload have been observed with exercise.[17] The authors speculate that this could be due to a loss of cardiomyocyte reserve because of an increased state of activation at baseline. Here, we deliver experimental evidence further strengthening this hypothesis. In our mouse model, cardiomyocyte contractility is enhanced at rest—possibly to compensate for altered afterload—which limits the adrenergic reserve leading to a loss of cardiac output reserve with adrenergic stimuli.

Last, we investigated molecular pathways contributing to the hypercontractile cardiomyocyte state. In accordance with a largely preserved absolute cardiomyocyte response to adrenergic stimuli, we did not find a reduction of β1-AR on the outer cardiomyocyte membrane. These findings are fundamentally different from HFrEF and from findings in insulin-challenged cardiomyocytes,[32] potentially contributing to the understanding of the ineffectiveness of beta blockers in HFpEF patients.[33] Previous evidence has demonstrated increased S-nitrosylation as an upstream driver of HFpEF which could be improved by genetic or pharmacologic inhibition of nNOS or iNOS.[7,8] We found that nNOS inhibition was able to reduce NO synthesis in control and HFpEF. However, iNOS inhibition only reduced NO synthesis in HFpEF, further supporting its specific upregulation in HFpEF. We also found increased ROS production in HFpEF that has been shown to reroute the effect of NO from the cyclic GMP—protein kinase G signaling pathway toward S-nitrosylation.[6] It is known that S-nitrosylation enhances cellular relaxation via direct upregulation of the activity of SERCA2 and inhibition of phospholamban.[5,6] Accordingly, we observed a slowing of cardiomyocyte relaxation with inhibitors of nNOS, iNOS, and with glutathione which was pronounced in HFpEF. However, S-nitrosylation of sarcomeric proteins was demonstrated to reduce the myofilament's sensitivity to calcium.[6] The increase in calcium sensitivity we observed must therefore be caused by a different signaling pathway. Despite its detrimental effect on the ER stress response and fibrosis shown previously,[7,8] NO in our experiments seems

17481716, 0, Downloaded from https://onlinelibrary.wiley.com/doi/10.1111/apha.14124 by University Of St Andrews University, Wiley Online Library on [04/03/2024]. See the Terms and Conditions (https://onlinelibrary.wiley.com/terms-and-conditions) on Wiley Online Library for rules of use; OA articles are governed by the applicable Creative Commons License

to improve cardiomyocyte contractility and relaxation in HFpEF. This dual effect might constitute an example of antagonistic pleiotropy.

4 | MATERIALS AND METHODS

4.1 | Animal model of HFpEF

All experiments involving animals were performed according to the rules of and approved by the local authorities (approval no. G0104/20). Male C57BL6J mice were acquired from Charles River Laboratories. At the age of 12 weeks, mice were randomized to either a standard diet (Rat/Mouse Maintenance V1534, sniff Spezialdiäten, Soest, Germany) and drinking water or high-fat diet (D12492, Research Diet Inc.) and 1 g/L L-NAME (N5751, Sigma-Aldrich) in the drinking water for 15 weeks. All following experiments were performed in the 15th week of treatment. Of the 20 mice in each group, 4 HFpEF mice died between 23 and 27 weeks of age due to unknown causes. For a subset of experiments, we used 23-week-old Wistar Kyoto or obese Zucker fatty and spontaneously hypertensive (ZSF1) rats. For detailed information on the procedures in these animals see Bode et al.[34]

4.2 | Echocardiography and stress echocardiography

Transthoracic echocardiography was performed on a Visualsonic Vevo 3100 (Visual Sonic) in awake, gently restrained mice.[35] For systolic function and LV geometry, M- and B-mode images were recorded from the parasternal short axis at the papillary muscle level. For the assessment of diastolic function, pulse wave Doppler of mitral valve inflow (E) and peak mitral annular tissue Doppler velocity during early filling (e′) were recorded from the parasternal long-axis view.

Both timepoints of stress echocardiography were performed in anesthetized (isoflurane, 1.5%–2%, heart rate of 400 to 450 bpm) mice. Systolic function was assessed using M-Mode images in the parasternal long-axis view. Then, mice were injected intraperitoneally with Iso at a dose of 0.6 μg/g body weight in 100 μL phosphate-buffered saline. Systolic function was reassessed 90 s after injection when the heart rate reached a stable plateau.

All echocardiography image analysis was performed in VevoLab (V. 5.6.1). For a subset of experiments, B-mode images acquired from the parasternal long axis view were used to calculate longitudinal strain using the VevoStrain software and a speckle-tracking algorithm. The epi- and endocardial wall was traced manually, strain analysis was performed, and longitudinal strain was calculated for six anatomical regions and then averaged.

4.3 | Exercise testing

Exercise testing was performed on a treadmill (TSE systems). The system was set at a constant angle of 20° and the running speed was increased stepwise: 3 min 0 m/s, 2 min 0.1 m/s, 2 min 0.2 m/s, 2 min 0.23 m/s, 2 min 0.26 m/s, 2 min 0.3 m/s, 2 min 0.35 m/s, 2 min 0.4 m/s, 6 min 0.45 m/s. We measured the time to exhaustion and the distance run by each animal. Exhaustion was defined as not returning to running after having been pushed back onto the treadmill three times.

4.4 | Chemicals and solutions

All chemicals were obtained from Sigma-Aldrich if not noted otherwise. Normal Tyrode solution (NT) contained (mM): 136 NaCl, 4 KCl, 1 $CaCl_2$, 1 $MgCl_2$, 10 Glucose, 10 HEPES, 0.2 L-arginine; pH adjusted to 7.4 with NaOH. A subset of experiments was conducted in NT solution with 3 mM calcium (NT3). Tyrode solution without calcium and sodium (0Na0Ca) contained (mM): 130 LiCl, 4 KCl, 1 $MgCl_2$, 10 glucose, and 10 HEPES, pH adjusted to 7.4 with LiOH.

4.5 | Isolation of adult, left ventricular cardiomyocytes

AVCMs were isolated from mouse hearts as previously described.[36] In short, mouse hearts were excised, transferred to cold buffer (1.8 mM Ca), secured on a cannula and retrogradely perfused on a Langendorff apparatus at 36°C. After 2 min of calcium free buffer, the solution was switched to enzyme-containing buffer (Liberase, Sigma-Aldrich, 120 μg/mL) for 6 to 7 min. LV tissue was dissected in low calcium buffer (12.5 μM), gently dispersed and cells were allowed to settle, transferred into NT solution and the calcium concentration was increased stepwise to 1 mM. All cardiomyocyte experiments were performed within 4 h after isolation. Isolation of AVCMs was performed on 14 control mice und 12 HFpEF mice hearts. The procedure failed to provide high quality cardiomyocytes (evaluated as number of cardiomyocytes and percentage of viable cardiomyocytes) three times in each group resulting in a final sample size of 11 versus 9 in control versus HFpEF respectively.

17481716, 0, Downloaded from https://onlinelibrary.wiley.com/doi/10.1111/apha.14124 by University Of St Andrews University, Wiley Online Library on [04/03/2024]. See the Terms and Conditions (https://onlinelibrary.wiley.com/terms-and-conditions) on Wiley Online Library for rules of use; OA articles are governed by the applicable Creative Commons License

4.6 | Ratiometric calcium imaging and sarcomere shortening

AVCMs were plated on laminin-coated, glass-bottom dishes in NT solution with Fura-2 AM (Thermo Fisher Scientific, Waltham, MA, USA) at 1 μM for 20 min with 0.02% pluronic F127, followed by 20 min in dye-free solution to wash-out non-esterified residues of the dye. Dishes were mounted on a ratiometric microscope (CytoCypher MultiCell System, CytoCypher BV, Netherlands), cells were placed in NT with 1.8 mM calcium, electrically stimulated at 1 Hz for at least 4 min to reach a steady state (Myopacer, Ionoptix) and Ca^{2+}-dependent fluorescence (excitation at 340 and 385 nm, emission collected at 510 ± 40) and sarcomere shortening (optical channel) were recorded for 7 s at 35°C in Ionwizard (V7.15.1.162, Ionoptix). Sarcomere and calcium traces were analyzed using the Transient Analysis Tool (Ionoptix). Analysis in this tool runs on raw, non-filtered traces. Background fluorescence was assessed at the beginning of each experiment, was less than 15% of the absolute fluorescence, and was not subtracted. All cardiomyocyte data were averaged per protocol and animal. At least five cardiomyocytes were measured for each animal in each protocol.

For a subset of experiments, AVCMs were measured once, then Iso (1 μM) or SNAP (10 μM) were added, and the same cells were recorded a second time after 5 min. For all repeated measurements, the second measurement was corrected for the change in background fluorescence. For another subset of experiments, AVCMs were preincubated with SMTC (a specific inhibitor of nNOS, 300 nM, Sigma-Aldrich, 40 min), 1400W (a specific inhibitor of iNOS, 1 μM, Sigma-Aldrich, 40 min) or a cell-permeable derivate of glutathione (0.5 mM, Sigma-Aldrich, 20 min) prior to imaging.

4.7 | Confocal calcium imaging

AVCMs were plated on laminin-coated, glass-bottom dishes and washed with NT solution with 1 mM calcium after 10 min of attachment, loaded with 2 μM of the calcium-sensitive dye Fluo-4 AM (Thermo Fisher Scientific) in NT1 with 0.05% Pluronic®F-127 for 20–30 min at room temperature followed by washing with NT3 solution. Stained AVCMs were placed under a confocal microscope (LSM810, Carl Zeiss) equipped with a perfusion system and a stimulator (Ionoptix). Linescan images were recorded longitudinally through the whole cell with a length of 512 pixels. AVCMs were stimulated at 1 Hz to reach a stable steady state in NT3 and a representative 10 s segment was recorded. Then the perfusion was changed to 0 Na/0 Ca solution and the electrical pacing was terminated to record spontaneous intracellular calcium release events for 14 s. We then restarted NT3, perfused the cells with caffeine (30 mM), and recorded the caffeine-induced calcium transient.

Ca^{2+}-dependent fluorescence intensity (F) along the scan line was averaged to obtain the global Ca^{2+}-transient and then normalized to the diastolic fluorescence intensity (F/F_0). Amplitude, time to half-maximal, and maximal Ca^{2+} were calculated. A monoexponential curve was fitted to the calcium decay (starting at 90% amplitude following the peak) and the decay constant (tau) was calculated. During the phase of transfusion with 0Na0Ca solution, CaREv was quantified.

4.8 | Fluorescence correlation spectroscopy of β_1 adrenergic receptor density at the cardiomyocyte outer membrane

Fluorescence correlation spectroscopy measurements were conducted on isolated AVCMs as previously described.[37] Briefly, receptors were labeled with a fluorescently tagged inverse agonist (Carazolol), and line scans were conducted on AVCMs in a Leica SP8 confocal microscope at a rate of 1.4 kHz for approximately 500k lines. The resulting kymographs were spatially and temporally correlated to obtain a 2-dimensional correlation function referred to as the STICS function.[38] The profile of this function at space lag (0) was used to extract a single-point correlation function and fit. Data were fit to the following equation to obtain the number of fluorescent molecules (=receptors) in the excitation volume: $G(\text{tau}) = 0.35/N * (1 + 4D * \text{tau}/w_{xz}^2)^{-1}$, where D is the diffusion coefficient, and w_{xz} is the waist of the excitation volume of the confocal microscope in the x–z plane.

4.9 | Reactive oxygen species and NO measurements

The previously well characterized NO-specific fluorescence dye NO–ON (1 mM in DMSO, Strem chemicals, Newburyport, MA)[11] was mixed with $CuCl_2$ (1 mM) at 1:2 ratio and loaded into AVCMs at 1 μM at room temperature for 2 h. The ROS probe 2′,7′-dichlorodihydrofluorescein (DCF, Thermo Fisher Scientific) was loaded into AVCMs at 10 μM at room temperature for 45 min. After dye loading, cells were washed and plated on laminin-coated 24-well plates at a density of approx. 1000 living cardiomyocytes per well in NT with 1.8 mM calcium and then washed again to remove dead cells. All wells were imaged at the experiment's start, and the data were normalized to this initial fluorescence to account for variations in the number of AVMC. For a subset of experiments, cells

17481716, 0, Downloaded from https://onlinelibrary.wiley.com/doi/10.1111/apha.14124 by University Of St Andrews University, Wiley Online Library on [04/03/2024]. See the Terms and Conditions (https://onlinelibrary.wiley.com/terms-and-conditions) on Wiley Online Library for rules of use; OA articles are governed by the applicable Creative Commons License

were incubated with elamipretide (10 μM, Sigma-Aldrich, 20 min) or SMTC or 1400 W (concentration and incubation time as described above). Imaging was conducted on a Cytofluor II (Applied Biosystems). Excitation was set to 485 nm + −10 nm, and emission was collected at 530 nm + −12.5 nm with a gain of 65 V (NO-ON) or 75 V (DCF). For a subset of experiments, 1 μM Iso was added and cells were reimaged after 5 min. For a subset of experiments, cells were stimulated electrically at 1 or 3 Hz (Myopacer, Ionoptix) using a platinum wire adapter for 24 well plates for 5 min between measurements. For each experimental condition, data were calculated by subtracting the initial fluorescence from the final fluorescence in that condition and then dividing by the initial fluorescence of that well. For all plate reader experiments, at least four replicates per group were conducted and outliers were identified using the boxplot method (>3. quartile +1.5 * [3. quartile − 1 quartile] or <1. quartile − 1.5 * [3. quartile − 1. quartile]) and removed for final analysis.

4.10 | Western blotting

Left ventricular tissue was homogenized at 4°C in lysis buffer, containing (mM, if not stated otherwise): 20 Tris–HCl (pH 7.4), 137 NaCl, 20 NaF, 1 sodium pyrophosphate, 50 β-glycerophosphate, 10 EDTA, 1 EGTA, 1 PMSF, 10% glycerol, 1% NP 40, 4 μg/mL aprotinin, 4 μg/mL pepstatin A, and 4 μg/mL leupeptin. Protein concentration was determined via a BCA assay (#23225, Thermo Fisher Scientific, Waltham, MA, USA). In this study, 20 μg of protein was run on 4%–15% Bis–Tris polyacrylamide gels (16.5% Tris-Tricine for phospholamban) and transferred to nitrocellulose membranes. Proteins on the membrane were stained with a total protein stain (LI-COR, Lincoln, Nebraska USA). Blocking was conducted with 5% dried milk in Tris-buffered saline (pH 7.5) containing 0.1% Tween 20. Membranes were probed with anti-SERCA2a (1:1000, Santa Cruz, Heidelberg, Germany), anti-MYBPC3 (1:1000, Santa Cruz, Heidelberg, Germany), anti-phospho-Ser282 MYBPC3 (1:500, Enzo Life Sciences, Farmingdale, NY, USA), anti-Troponin I (1:1000, Novus Biologicals, Centennial, Colorado, USA), anti-phospho-Ser23/Ser24 Troponin I (1:1000, Cell Signaling, Danvers, Massachusetts, USA), anti-GAPDH (1:2000, Cell Signaling, Danvers, Massachusetts, USA), anti-phospho-Ser16 PLB (1:1000, Badrilla, Leeds, UK), and anti-PLB (1:1000, Santa Cruz, Heidelberg, Germany) overnight at 4°C. Anti-rabbit or Anti-mouse IgG linked with IRDye 680RD or IRDye 800RD (1:10 000, LI-COR, Lincoln, Nebraska, USA) were used as a secondary antibody. The signal was detected on an Odyssey CLx System and densitometry was performed using Image Studio software (LI-COR). All signals were normalized to GAPDH. Uncut images of the western blots can be found in Supporting Information Figure S6.

4.11 | Data analysis

All experiments and data analysis were conducted in accordance with the publishing guidelines in physiology.[39] All data analysis and statistics were performed in R (V 4.1.2). Data were analyzed per animal (except for Figures 3F,M,N and 5E–H, Supporting Information Figure S4C–I). Differences between the two groups were tested using a two-tailed, unpaired Student's *t*-test, Wilcoxon signed-rank test for non-normal data (as indicated by significant, groupwise Shapiro–Wilk test), or chi-squared test for categorial-dependent variables (Figure 3L). Repeated measure data were analyzed using mixed effect models. For the single cardiomyocyte data presented in Figure 5E–H and Supporting Information Figure S4C–I, we used a mixed linear model approach with the animal and the cell as random intercepts. All mixed models were fitted using the lme4 package (V 1.1-31) using optimization of REML criteria. We performed post-hoc testing calculating marginal means, estimating the degree of freedom using the Kenward-Rodger method and correcting pairwise post-hoc tests for multiple testing using the Sidak method per family. *p*-values below 0.05 were regarded as statistically significant.

5 | CONCLUSION

In HFpEF, the adrenergic reserve is impaired in vivo and left ventricular cardiomyocytes. In contrast to HFrEF, a hypercontractile phenotype at baseline and largely preserved maximal responses with adrenergic stimuli underly the defective reserve. Increased myofilament sensitivity and faster calcium reuptake underlie these alterations which are partially caused by a dysregulation of nitro-oxidative signaling. These findings emphasize the importance of adrenergic signaling in HFpEF both to explain the lack of benefit of well-established HFrEF therapies (e.g., beta blockers) as well as new therapeutic targets (e.g., nitro-oxidative signaling).

5.1 | Limitations

Besides its broad usage in the HFpEF community, the two-hit mouse model comes with limitations. Although our data on NO synthesis in HFpEF cardiomyocytes

17481716, 0, Downloaded from https://onlinelibrary.wiley.com/doi/10.1111/apha.14124 by University Of St Andrews University, Wiley Online Library on [04/03/2024]. See the Terms and Conditions (https://onlinelibrary.wiley.com/terms-and-conditions) on Wiley Online Library for rules of use; OA articles are governed by the applicable Creative Commons License

imply a small activity of L-NAME within cardiomyocytes, we cannot exclude that findings with NO synthase inhibitors (SMTC, 1400W) in cardiomyocytes were modified by the systemic administration of L-NAME. Additionally, this study does not elucidate whether these findings are sex specific. Further research in this direction is required.

AUTHOR CONTRIBUTIONS

Lukas Semmler: Conceptualization; investigation; formal analysis; project administration; writing – original draft; writing – review and editing. **Tobias Jeising:** Investigation; formal analysis. **Judith Huettemeister:** Investigation; formal analysis; writing – original draft; writing – review and editing. **Marc Bathe-Peters:** Investigation; formal analysis. **Konstantina Georgoula:** Investigation; formal analysis. **Rashin Roshanbin:** Investigation; formal analysis. **Paulina Sander:** Investigation; formal analysis; writing – review and editing. **Shu Fu:** Investigation; formal analysis. **David Bode:** Investigation; formal analysis. **Felix Hohendanner:** Funding acquisition; writing – original draft; writing – review and editing. **Burkert M. Pieske:** Funding acquisition. **Paolo Annibale:** Investigation; formal analysis; project administration; writing – review and editing. **Gabriele G. Schiattarella:** Investigation; formal analysis; funding acquisition. **Christian U. Oeing:** Investigation; formal analysis; writing – original draft; writing – review and editing; funding acquisition; project administration. **Frank R. Heinzel:** Conceptualization; funding acquisition; writing – original draft; writing – review and editing; project administration.

ACKNOWLEDGMENTS

We thank Silke Stanislawiak for her assistance. Open Access funding enabled and organized by Projekt DEAL.

FUNDING INFORMATION

This project is funded by grants from the Deutsche Forschungsgemeinschaft (DFG, German Research Foundation—SFB 1470—A01 to FRH and PA and A02 to GGS) and from the DZHK (German Centre for Cardiovascular Research to GGS). CUO is additionally funded by the DFG (OE 688/4-1).

CONFLICT OF INTEREST STATEMENT

The authors declare no conflict of interest.

DATA AVAILABILITY STATEMENT

The data that support the findings of this study are available from the corresponding author upon reasonable request.

ORCID

Lukas Semmler https://orcid.org/0000-0003-2933-7566
Christian U. Oeing https://orcid.org/0000-0002-0816-4443
Frank R. Heinzel https://orcid.org/0000-0002-4529-5282

REFERENCES

1. Kavanagh T, Mertens DJ, Hamm LF, et al. Prediction of long-term prognosis in 12 169 men referred for cardiac rehabilitation. *Circulation*. 2002;106(6):666-671.
2. Pandey A, Khera R, Park B, et al. Relative impairments in hemodynamic exercise reserve parameters in heart failure with preserved ejection fraction: a study-level pooled analysis. *JACC Heart Fail*. 2018;6(2):117-126.
3. Mesquita T, Zhang R, Cho JH, et al. Mechanisms of sinoatrial node dysfunction in heart failure with preserved ejection fraction. *Circulation*. 2022;145(1):45-60.
4. Harding SE, Jones SM, O'Gara P, del Monte F, Vescovo G, Poole-Wilson PA. Isolated ventricular myocytes from failing and non-failing human heart; the relation of age and clinical status of patients to isoproterenol response. *J Mol Cell Cardiol*. 1992;24(5):549-564.
5. Irie T, Sips PY, Kai S, et al. S-Nitrosylation of calcium-handling proteins in cardiac adrenergic signaling and hypertrophy. *Circ Res*. 2015;117(9):793-803.
6. Vielma AZ, León L, Fernández IC, González DR, Boric MP. Nitric oxide synthase 1 modulates basal and beta-adrenergic-stimulated contractility by rapid and reversible redox-dependent S-nitrosylation of the heart. *PLoS ONE*. 2016;11(8):e0160813.
7. Schiattarella GG, Altamirano F, Tong D, et al. Nitrosative stress drives heart failure with preserved ejection fraction. *Nature*. 2019;568(7752):351-356.
8. Yoon S, Kim M, Lee H, et al. S-Nitrosylation of histone deacetylase 2 by neuronal nitric oxide synthase as a mechanism of diastolic dysfunction. *Circulation*. 2021;143(19):1912-1925.
9. Curl CL, Danes VR, Bell JR, et al. Cardiomyocyte functional etiology in heart failure with preserved ejection fraction is distinctive-a new preclinical model. *J Am Heart Assoc*. 2018;7(11):e007451.
10. Hohendanner F, Bode D, Primessnig U, et al. Cellular mechanisms of metabolic syndrome-related atrial decompensation in a rat model of HFpEF. *J Mol Cell Cardiol*. 2018;115:10-19.
11. Lim MH, Xu D, Lippard SJ. Visualization of nitric oxide in living cells by a copper-based fluorescent probe. *Nat Chem Biol*. 2006;2(7):375-380.
12. Stomberski CT, Hess DT, Stamler JS. Protein S-nitrosylation: determinants of specificity and enzymatic regulation of S-nitrosothiol-based signaling. *Antioxid Redox Signal*. 2019;30(10):1331-1351.
13. Kavoussi PK, Smith RP, Oliver JL, et al. S-nitrosylation of endothelial nitric oxide synthase impacts erectile function. *Int J Impot Res*. 2019;31(1):31-38.
14. Santos M, Opotowsky AR, Shah AM, Tracy J, Waxman AB, Systrom DM. Central cardiac limit to aerobic capacity in patients with exertional pulmonary venous hypertension:

17481716, 0, Downloaded from https://onlinelibrary.wiley.com/doi/10.1111/apha.14124 by University Of St Andrews University, Wiley Online Library on [04/03/2024]. See the Terms and Conditions (https://onlinelibrary.wiley.com/terms-and-conditions) on Wiley Online Library for rules of use; OA articles are governed by the applicable Creative Commons License

implications for heart failure with preserved ejection fraction. *Circ Heart Fail*. 2015;8(2):278-285.
15. Montero D, Diaz-Canestro C. Determinants of exercise intolerance in heart failure with preserved ejection fraction: a systematic review and meta-analysis. *Int J Cardiol*. 2018;254:224-229.
16. Dhakal BP, Malhotra R, Murphy RM, et al. Mechanisms of exercise intolerance in heart failure with preserved ejection fraction: the role of abnormal peripheral oxygen extraction. *Circ Heart Fail*. 2015;8(2):286-294.
17. Rosch S, Kresoja KP, Besler C, et al. Characteristics of heart failure with preserved ejection fraction across the range of left ventricular ejection fraction. *Circulation*. 2022;146(7):506-518.
18. Kawaguchi M, Hay I, Fetics B, Kass DA. Combined ventricular systolic and arterial stiffening in patients with heart failure and preserved ejection fraction: implications for systolic and diastolic reserve limitations. *Circulation*. 2003;107(5):714-720.
19. Rommel KP, von Roeder M, Latuscynski K, et al. Extracellular volume fraction for characterization of patients with heart failure and preserved ejection fraction. *J Am Coll Cardiol*. 2016;67(15):1815-1825.
20. Houser SR, Piacentino V 3rd, Weisser J. Abnormalities of calcium cycling in the hypertrophied and failing heart. *J Mol Cell Cardiol*. 2000;32(9):1595-1607.
21. Tarazi RC, Levy MN. Cardiac responses to increased afterload. State-of-the-art review. *Hypertension*. 1982;4(3 pt 2):8-18.
22. Heinzel FR, Hegemann N, Hohendanner F, et al. Left ventricular dysfunction in heart failure with preserved ejection fraction-molecular mechanisms and impact on right ventricular function. *Cardiovasc Diagn Ther*. 2020;10(5):1541-1560.
23. Hamdani N, Franssen C, Lourenço A, et al. Myocardial titin hypophosphorylation importantly contributes to heart failure with preserved ejection fraction in a rat metabolic risk model. *Circ Heart Fail*. 2013;6(6):1239-1249.
24. Frisk M, le C, Shen X, et al. Etiology-dependent impairment of diastolic cardiomyocyte calcium homeostasis in heart failure with preserved ejection fraction. *J Am Coll Cardiol*. 2021;77(4):405-419.
25. Miranda-Silva D, Wüst RCI, Conceição G, et al. Disturbed cardiac mitochondrial and cytosolic calcium handling in a metabolic risk-related rat model of heart failure with preserved ejection fraction. *Acta Physiol (Oxf)*. 2020;228(3):e13378.
26. Kilfoil PJ, Lotteau S, Zhang R, et al. Distinct features of calcium handling and beta-adrenergic sensitivity in heart failure with preserved versus reduced ejection fraction. *J Physiol*. 2020;598(22):5091-5108.
27. Olver TD, Edwards JC, Jurrissen TJ, et al. Western diet-fed, aortic-banded Ossabaw swine: a preclinical model of cardio-metabolic heart failure. *JACC Basic Transl Sci*. 2019;4(3):404-421.
28. van Heerebeek L, Borbély A, Niessen HWM, et al. Myocardial structure and function differ in systolic and diastolic heart failure. *Circulation*. 2006;113(16):1966-1973.
29. Leite-Moreira AF, Correia-Pinto J, Gillebert TC. Afterload induced changes in myocardial relaxation: a mechanism for diastolic dysfunction. *Cardiovasc Res*. 1999;43(2):344-353.
30. Popovic D, Alogna A, Omar M, et al. Ventricular stiffening and chamber contracture in heart failure with higher ejection fraction. *Eur J Heart Fail*. 2023;25:657-668.
31. Borlaug BA. Mechanisms of exercise intolerance in heart failure with preserved ejection fraction. *Circ J*. 2014;78(1):20-32.
32. Fu Q, Xu B, Parikh D, Cervantes D, Xiang YK. Insulin induces IRS2-dependent and GRK2-mediated beta2AR internalization to attenuate betaAR signaling in cardiomyocytes. *Cell Signal*. 2015;27(3):707-715.
33. Palau P, Seller J, Domínguez E, et al. Effect of beta-blocker withdrawal on functional capacity in heart failure and preserved ejection fraction. *J Am Coll Cardiol*. 2021;78(21):2042-2056.
34. Bode D, Semmler L, Wakula P, et al. Dual SGLT-1 and SGLT-2 inhibition improves left atrial dysfunction in HFpEF. *Cardiovasc Diabetol*. 2021;20(1):7.
35. Oeing CU, Jun S, Mishra S, et al. MTORC1-regulated metabolism controlled by TSC2 limits cardiac reperfusion injury. *Circ Res*. 2021;128(5):639-651.
36. Sedej S, Heinzel FR, Walther S, et al. Na+−dependent SR Ca2+ overload induces arrhythmogenic events in mouse cardiomyocytes with a human CPVT mutation. *Cardiovasc Res*. 2010;87(1):50-59.
37. Bathe-Peters M, Gmach P, Boltz HH, et al. Visualization of beta-adrenergic receptor dynamics and differential localization in cardiomyocytes. *Proc Natl Acad Sci USA*. 2021;118(23):e2101119118.
38. Bathe-Peters M, Gmach P, Annibale P, Lohse MJ. Linescan microscopy data to extract diffusion coefficient of a fluorescent species using a commercial confocal microscope. *Data Brief*. 2020;29:105063.
39. Jensen BL, Persson PB. Good publication practice in physiology 2021. *Acta Physiol (Oxf)*. 2022;234(1):e13741.

SUPPORTING INFORMATION

Additional supporting information can be found online in the Supporting Information section at the end of this article.

How to cite this article: Semmler L, Jeising T, Huettemeister J, et al. Impairment of the adrenergic reserve associated with exercise intolerance in a murine model of heart failure with preserved ejection fraction. *Acta Physiol*. 2024;00:e14124. doi:10.1111/apha.14124

17481716, 0, Downloaded from https://onlinelibrary.wiley.com/doi/10.1111/apha.14124 by University Of St Andrews University, Wiley Online Library on [04/03/2024]. See the Terms and Conditions (https://onlinelibrary.wiley.com/terms-and-conditions) on Wiley Online Library for rules of use; OA articles are governed by the applicable Creative Commons License